CHEMMEDCHEM

ChemPubSoc Europe

DOI: 10.1002/cmdc.201100560

VIP

Fluorogenic Peptide-Based Substrates for Monitoring Thrombin Activity

Sander S. van Berkel,[a] Bas van der Lee,[a] Floris L. van Delft,[a] Rob Wagenvoord,[b] H. Coenraad Hemker,[b] and Floris P. J. T. Rutjes*[a]

The synthesis of a series of peptides containing C-terminal 7-amino-4-methylcoumarin (AMC) for use in the thrombin generation test (TGT) is described. The lead structure in this project was H-Gly-Gly-Arg-AMC, of which the water solubility and kinetic parameters (K_M and k_{cat}) are greatly improved over those of the substrate in current use in the TGT: Cbz-Gly-Gly-Arg-AMC. A series of N-terminally substituted Gly-Gly-Arg-AMC derivatives were synthesized, as well as implementation of structural changes at either the P_2 or P_3 position of the peptide backbone. Furthermore, two substrates were synthesized that have structural similarities to the chromogenic thrombin substrate SQ68 or that contain a 1,2,3-triazole moiety in the peptide chain, mimicking an amide bond. To determine the applicability of newly synthesized fluorogenic substrates for monitoring continuous thrombin generation, the K_M and k_{cat} values of the conversion of these fluorogenic substrates by thrombin (FIIa) and factor Xa (FXa) were quantified. An initial selection was made on basis of these data, and suitable substrates were further evaluated as substrates in the thrombin generation assay. Assessment of the acquired data showed that several substrates, including the SQ68 derivative Et-malonate-Gly-Arg-AMC and N-functionalized Gly-Gly-Arg-AMC derivatives, are suitable candidates for replacement of the substrate currently in use.

Introduction

Thrombosis is responsible for such diseases as cerebral and coronary infarction and pulmonary embolism; moreover, it is considered a major cause of morbidity and mortality in the western world.[1] Two types of thrombosis are known: 1) arterial thrombosis, occurring in arteries, which can result in myocardial arrest (heart attack) or cerebral infarction (stroke), and 2) venous thrombosis, most commonly in the form of deep-vein thrombosis (DVT) occurring in the veins of the legs which can result in pulmonary embolism. Treatment of DVT is focused mainly on the prevention of clot growth, clot arrest, and avoiding the recurrence of clots via the inhibition of clotting factors. DVT is generally treated with anticoagulants such as immediate-acting heparin (either unfractionated heparin (UFH), low-molecular-weight heparin (LMWH), or the synthetic heparin fondaparinux) or slow-onset oral anticoagulants such as warfarin and rivaroxaban. Treatment of patients suffering from coronary or cerebral infarction is directed mainly toward platelet inhibition by medications such as aspirin, clopidogrel, and tirofiban.[2,3]

Because thrombin plays a pivotal role in pathological disturbances of the haemostatic system, inhibition of this enzyme may lead to useful treatments for thrombotic disorders. Understanding the crucial role of thrombin in blood coagulation and elucidation of the thrombin active site by X-ray crystallography[4] greatly facilitated researchers in developing direct thrombin inhibitors such as argatroban, melagatran, and ximelagatran.[5] The central function of thrombin in clot formation makes it a prime target for the design of antithrombotic drugs.[6] Structure–activity relationship (SAR) studies and parallel synthesis have led to the development of an array of novel thrombin inhibitors. Nonetheless, the antithrombotic agents in current clinical use possess a number of limitations such as the need for constant monitoring to assure effective drug levels in the plasma, and avoidance of bleeding complications and secondly potential drug–drug interactions.

The diagnostics of haemostatic and thrombotic (H&T) diseases, the control of antithrombotic and substitution therapy, and the development of new antithrombotics are all put at a disadvantage by the absence of an adequate test for the H&T system. Clotting time tests such as prothrombin time (PT)[7] and activated partial thromboplastin time (aPTT)[8] are frequently used as routine assessments of the blood's coagulation capacity. However, measuring clotting times—indicative for the moment of onset of thrombin generation—does not indicate hypercoagulability and is insensitive to mild bleeding disorders. This is emphasized by the fact that 95% of the thrombin formation responsible for hypercoagulation occurs after clot formation.[9] Other techniques used for monitoring haemostatic system function are thromboelastography[10] (TEG, which measures the mechanical properties of a clotting

[a] Dr. S. S. van Berkel, B. van der Lee, Dr. F. L. van Delft, Prof. Dr. F. P. J. T. Rutjes
Radboud University Nijmegen, Institute for Molecules and Materials
Heyendaalseweg 135, 6525 AJ Nijmegen (The Netherlands)
E-mail: F.Rutjes@science.ru.nl

[b] Dr. R. Wagenvoord, Prof. Dr. H. C. Hemker
Synapse BV, University of Maastricht
Cardiovascular Research Institute Maastricht
P.O. Box 616, 6200 MD Maastricht (The Netherlands)

Supporting information for this article is available on the WWW under http://dx.doi.org/10.1002/cmdc.201100560.

medium) and the use of a platelet function analyzer (PFA).[11] These techniques, however, do not reflect the overall functioning of the H&T system either, and are more suitable for determining other specific aspects of coagulation.[12] By far the most information on the function of the H&T system is gained by assessing the thrombin generation curve (TGC, or thrombogram, Figure 1), that is, the course of the thrombin concentration as

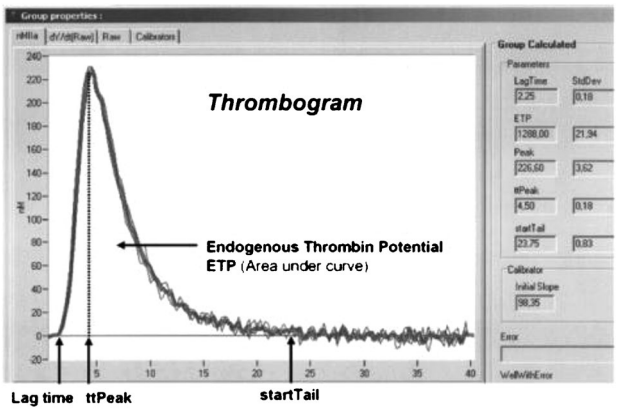

Figure 1. Real-time display of a thrombogram.

it develops in clotting blood or plasma. In contrast to clotting times, a thrombogram measures both low and high reactivity of the clotting system and is sensitive to the action of all types of antithrombotic drugs.[13–15] Monitoring the coagulation behavior of blood is therefore of utmost importance, firstly to detect the propensity of a patient to develop such disorders, and secondly to monitor the effectiveness of medication during treatment at a later stage if necessary.

The concept of measuring thrombin generation dates back to 1953 when it was simultaneously described by Macfarlane and Biggs,[16] and Pitney and Dacie.[17] The developed method required extraordinary skill and was highly time consuming. Hemker and co-workers therefore modified the classical approach by semi-automatically assessing the thrombin content of subsamples spectrophotometrically.[18] During the 1990s the subsampling approach was modified by adding a thrombin-specific substrate[19] with a low turnover number directly to the plasma and deriving the thrombin concentration in the plasma from the rate of substrate conversion.[20] This substrate, either SQ68[21] or S2238 (Figure 2), exhibited optimal kinetic parameters in terms of thrombin binding (K_M) and rate of hydrolysis (k_{cat}) and displayed no inhibitory activity against the prothrombinase complex or other coagulation factors. However, this method suffers from the significant restriction that optical density measurements must be performed on optically clear media.

Consequently, complete removal of fibrinogen and blood cells from plasma was required, eliminating the recognition of any effect of fibrin and/or platelets on thrombin generation. The importance of measuring thrombin generation in platelet-rich plasma (PRP) is undisputed, as platelets are the physiological source of the phospholipids required for thrombin activation.[22] Therefore, further research in this field led to the complete replacement of the initially used chromogenic substrates by a second-generation fluorogenic substrate, Cbz-Gly-Gly-Arg-AMC (**1**, Figure 2), which is currently in use for determining thrombin generation.[13] The main advantage of a fluorophore-based substrate is that the fluorescence signal is not disrupted by the inevitable increase in optical turbidity during measurement due to fibrin formation. Thrombin generation can thus be measured in both platelet-poor and platelet-rich plasma,[23] as well as in whole blood.[24] With the use of a fluorogenic substrate, another problem was encountered: the nonlinear correlation between the fluorescence signal and thrombin activity. This problem was overcome by monitoring substrate cleavage and comparing it with a constant known thrombin activity in a parallel nonclotting sample using calibrated automated thrombography.[25]

The use of fluorogenic peptide substrates was first reported by Zimmerman and co-workers, who employed peptides containing 7-amino-4-methylcoumarin (AMC) for assessment of the activity of various proteases and peptidases.[26] This concept led to the widespread application of AMC-containing peptides for monitoring the activity of aminopeptidase,[27] dipeptidase,[28] and carboxypeptidases.[29] Sakakibara et al. were among the first to report specific and sensitive peptide-AMC substrates for coagulation-related proteins such as thrombin and factor Xa,[30,31] activated protein C (APC),[32] and plasmin.[33] More recently, fluorogenic substrate libraries for the determination of protease specificity were produced by the research groups of Edwards and Ellman.[34,35] The above-mentioned re-

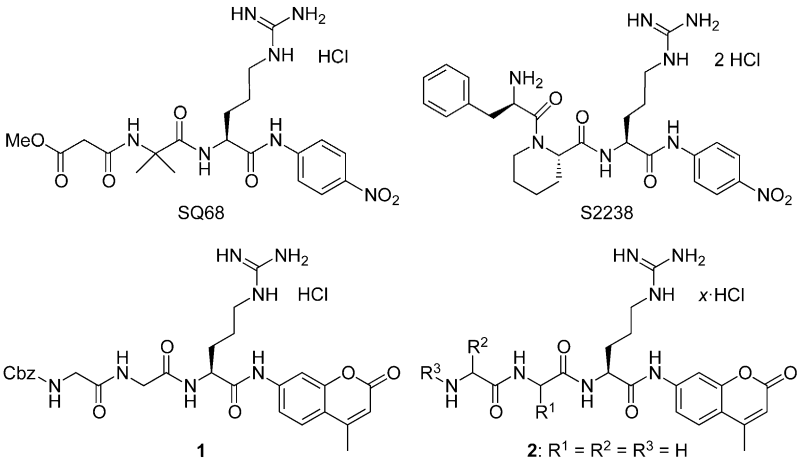

Figure 2. Structures of chromogenic substrates SQ68 and S2238 and the fluorogenic substrates Cbz-Gly-Gly-Arg-AMC (**1**) and derivative H-Gly-Gly-Arg-AMC·2 HCl (**2**).

search efforts, however, focused mainly on the discovery of specific and rapidly hydrolyzed protease substrates. Conversely, the thrombin generation method requires a substrate that is slowly hydrolyzed by thrombin to prevent substrate exhaustion before thrombin generation is complete, even at high substrate concentrations. The number of publications describing the synthesis and use of such slow-reacting thrombin-specific fluorogenic peptide substrates is, however, extremely limited.[36] In addition, the commercially available fluorogenic substrate **1** leaves substantial room for improvement, considering its moderate kinetic parameters and its poor solubility in water, which is clearly the solvent of choice for mimicking physiological conditions. Therefore, we describe herein the development of thrombin-specific substrates with increased aqueous solubility and improved kinetic parameters. We discuss our synthetic endeavors, biological evaluations, and the use of these substrates in the thrombin generation test (TGT).

Results and Discussion

Chemistry

With the poor water solubility of commercially available Cbz-Gly-Gly-Arg-AMC (**1**)[37] being its worst feature, initial studies were directed toward a seemingly straightforward carbobenzyloxy (Cbz) deprotection to obtain H-Gly-Gly-Arg-AMC (**2**). This was accomplished by the use of palladium on carbon (5 mol%) under an atmosphere of hydrogen in deuterated methanol. Unfortunately, N-deprotection to the desired product was accompanied by the formation of a by-product resulting from partial hydrogenation of the double bond of the AMC fragment. Using hydrogen bromide (33 wt% in acetic acid) also resulted in rapid product formation. However, hydrolysis of the Arg–AMC bond appeared to be a severe side reaction. Consequently, a Boc-protection peptide synthesis strategy was designed allowing deprotection of the Boc group under acidic conditions in the last step. A straightforward four-step synthesis, depicted in Scheme 1, provided compound **2** in a satisfactory 40% overall yield.

The critical step in the synthesis of compound **2** is the coupling of Boc-protected arginine with the fluorescent label AMC. Various published procedures describe methods involving a protection–deprotection strategy for the guanidine moiety of the arginine side chain.[38] A more straightforward approach, however, would entail the coupling of AMC to side chain unprotected Boc–arginine, which was pursued by applying a modified procedure described by Rijkers et al.[39] To this end, a mixture of Boc–arginine and AMC in pyridine at −15 °C was treated with phosphoryl chloride. Much to our satisfaction, Boc-Arg-AMC (**3**) was obtained in 68% yield after purification.[40] Subsequent deprotection of the Boc moiety resulted in the formation of product **4** in 94% yield. The coupling of Boc-Gly-Gly-OH with H-Arg-AMC·2 HCl (**4**) was achieved by using a standard peptide coupling method,[41] leading to the desired product **5** in good yield (83%). The final step comprised Boc deprotection of **5** to afford the desired tripeptide **2** as a hydrochloride salt in 96% yield.

Next, a series of N-terminus-substituted derivatives (**6**–**12**, Scheme 2) based on the tripeptide H-Gly-Gly-Arg-AMC (**2**) were synthesized to study the influence of N-terminal substituents. Various methods were applied for the introduction of substituents at the N-terminus of compound **2**. N-Terminal modification with acetyl, ethylsulfonyl, and ethoxycarbonyl substituents was carried out by using the corresponding chlorides and triethylamine in an appropriate solvent (Table 1, Entries 1–3). In all cases the use of one equivalent of the acid- or sulfonyl chloride was insufficient for complete conversion into the desired product. Therefore, an additional equivalent was added, and reaction times were prolonged. This led to full conversion; however, small amounts of di- and trisubstituted products were also obtained in the synthesis of compounds **7** and **8**. Introduction of a trifluoroacetyl group at the N-terminus was achieved with trifluoroacetic acid anhydride in dioxane in the presence of triethylamine, resulting in compound **9** in reasonable yield (59%). The design of compounds **10**–**12** was based on their aromatic character (capable of binding in the aromatic pocket of thrombin) and/or hydrophilic disposition. Substrates **11** and **12** were readily obtained by using standard peptide synthesis techniques,[41] but the synthesis of compound **10** failed. The coupling of 2-furanoic acid to H-Gly-Gly-Arg-AMC gave com-

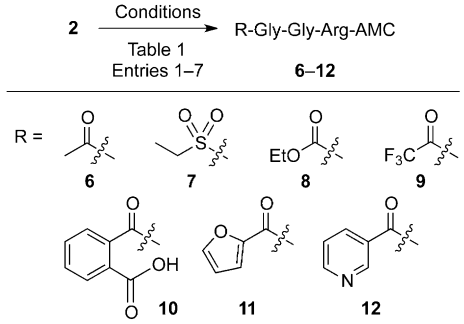

Scheme 2. Library synthesis of N-terminus-substituted H-Gly-Gly-Arg-AMC (**2**) derivatives **6**–**12**.

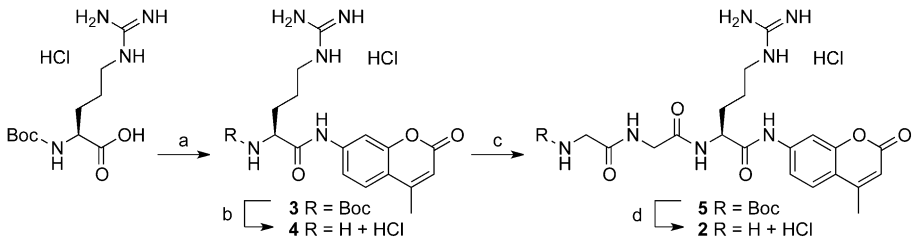

Scheme 1. Synthesis of H-Gly-Gly-Arg-AMC·2 HCl (**2**). *Reagents and conditions*: a) AMC, $POCl_3$, pyridine (dry), −15 °C→RT (68%); b) 2.6 M HCl in EtOAc, RT (94%); c) Boc-Gly-Gly-OH (1.02 equiv), DMF, EDC·HCl (1.1 equiv), DMAP (2 equiv), 0 °C→RT (86%); d) 2.6 M HCl in EtOAc, Et_2O, RT (98%).

Table 1. Reaction conditions applied for the preparation of compounds **6**–**12**.

Entry	Reagent	Conditions	Product	Yield [%][a]
1	AcCl	dioxane, Et_3N, RT, 72 h	**6**	47
2	$EtSO_2Cl$	MeCN, Et_3N, 45 °C, 4 h	**7**	68
3	EtO_2CCl	CH_2Cl_2, Et_3N, RT, 72 h	**8**	50
4	$(CF_3CO)_2O$	dioxane, Et_3N, RT, 18 h	**9**	59
5	phthalic anhydride	MeCN, Et_3N, RT, 16 h	**10**	0
6	2-furanoic acid	DMF, EDC, DMAP, RT, 16 h	**11**	35
7	nicotinic acid	DMF, EDC, DMAP, RT, 16 h	**12**	69

[a] Isolated yields after purification by countercurrent chromatography.

pound **11** in moderate yield (35%). Conversely, coupling of nicotinic acid and subsequent lyophilization from dilute aqueous hydrochloric acid gave compound **12** in good yield (69%). Most of the six obtained N-functionalized H-Gly-Gly-Arg-AMC derivatives showed good water solubility, with the exception of compounds **7** (poor) and **11** (moderate).

To investigate the influence of the amino acid at P_2 and P_3, we set out to synthesize a series of tripeptides containing small structural changes at these two positions (Scheme 3). In this study we kept the P_1 position constant, that is, arginine to ensure optimal interaction with the S_1 pocket. The residue at P_2 was systematically varied, incorporating glycine, valine, proline, or alanine residues, while maintaining alanine at the P_3 position. The peptide coupling conditions and deprotection procedure as described for compound **2** were subsequently employed in the synthesis of the tripeptide library (Scheme 3). The dipeptide H-Ala-Arg-AMC (**14**) was obtained in two steps, involving the coupling of H-Arg-AMC (**4**) with Boc-Ala-OH and subsequent Boc deprotection of the dipeptide **13**. The tripeptides **18**, **22**, and **26** were synthesized by a straightforward four-step reaction protocol. To obtain tripeptide H-Ala-Pro-Arg-AMC (**18**), dipeptide **21** was first produced in 60% yield over two steps. Subsequent coupling of the dipeptide fragment to H-Arg-AMC (**4**) and Boc deprotection using trifluoroacetic acid in dichloromethane resulted in compound **18** in 48% overall yield. The yield of compound **17** was not determined as a result of HOBt coordination to the arginine residue, so that the yield was calculated over two steps (a and b, 80%). A similar sequence was applied to obtain tripeptides H-Ala-Val-Arg-AMC (**22**) and H-Ala-Gly-Arg-AMC (**26**) in overall yields of 43 and 28%, respectively, over four steps. The overall yields of the Ala-containing peptides **14**, **18**, **22**, and **26** ranged from 28 to 80%.

Previous studies have shown that substrate SQ68 (Figure 2) possesses interesting kinetic properties suitable for the TGT.[20a,42] We therefore set out to synthesize a structurally similar compound, though bearing a fluorescent probe (AMC) instead of the *para*-nitroaniline chromophore (Scheme 4). The first step in the synthesis of SQ68 derivative **29** was the coupling of monoethyl malonate to *tert*-butyl-protected glycine to furnish compound **27**. Use of the glycine *tert*-butyl ester allowed selective acid-catalyzed deprotection of the *tert*-butyl ester without initiating hydrolysis of the ethyl ester. Performing the acid-catalyzed hydrolysis on *tert*-butyl ester **27** in the presence of trifluoroacetic acid generated compound **28** in good yield (84%). Subsequent coupling of H-Arg-AMC gave SQ68 mimic **29** in reasonable yield (66%) after countercurrent chromatography.

Further exploration of potential substrates for continuous thrombin generation led to the design of substrate **35**, replacing one of the peptide bonds in the substrate H-Gly-Gly-Arg-AMC (**2**) with a 1,2,3-triazole functionality. Previous studies suggest that these 1,2,3-triazole moieties might be perfect isosteres for peptide bonds[43] and that triazole mimics of biologically active substrates often retain their biological activity.[44] For that reason a 1,2,3-triazole was positioned between the two glycine residues of H-Gly-Gly-Arg-AMC, replacing the amide bond in order to investigate the kinetic effects of this substitution. Scheme 4 shows the synthetic pathway toward H-Gly-[triazole]-Gly-Arg-AMC (**35**). The synthetic procedure applied for the preparation of methyl 2-azidoacetate (**30**) involved reaction of methyl bromoacetate with sodium azide which resulted in the slightly volatile azide **30** in excellent yield (95%).

To obtain the triazole functionality, use of the copper-catalyzed 1,3-dipolar cycloaddition reaction[45] was envisioned. Although this reaction is robust and tolerant to many functional groups,[46] unprotected propargylamine appeared unsuited for the copper-

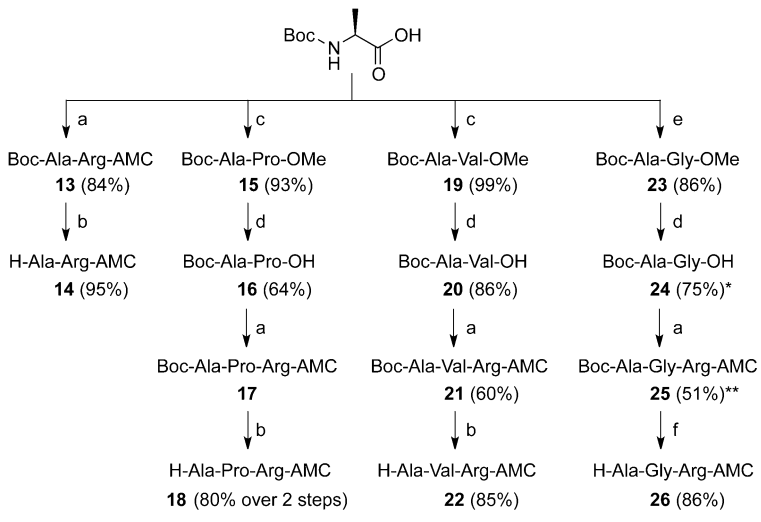

Scheme 3. Synthesis of Ala-containing peptide library. *Reagents and conditions*: a) H-Arg-AMC (**4**), DMF, EDC·HCl (1.1 equiv), DMAP (2 equiv), HOBt (1.0 equiv), 0 °C→RT; b) TFA, CH_2Cl_2, 0 °C→RT; c) H-AA-OMe, CH_2Cl_2, EDC·HCl (1.1 equiv), DiPEA (1.1 equiv), HOBt (1.0 equiv), 0 °C→RT; d) 1 M NaOH, THF, 0 °C→RT; e) H-Gly-OMe, EtOAc, DCC (1.05 equiv), NMM (1.1 equiv), HOBt (1.0 equiv), 0 °C→RT; f) 2.6 M HCl in EtOAc, Et_2O, RT. [*] 2 M NaOH instead of 1 M. [**] No HOBt added. AA = amino acid.

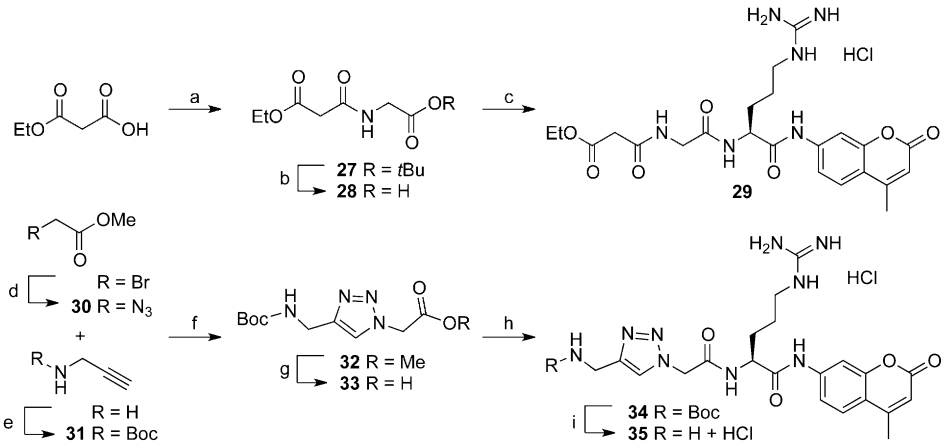

Scheme 4. Synthesis of Et-malonyl-Gly-Arg-AMC **29** and 1,2,3-triazole-containing fluorogenic substrate **35**. *Reagents and conditions*: a) H-Gly-O*t*Bu, CH_2Cl_2, EDC·HCl (1.1 equiv), DMAP (2 equiv), 0 °C→RT (58%); b) TFA, CH_2Cl_2, 0 °C→RT (84%); c) H-Arg-AMC (**4**), DMF, EDC·HCl (1.1 equiv), DMAP (2 equiv), 0 °C→RT (66%); d) NaN_3, DMF, RT, N_2 atmosphere (95%); e) Boc_2O, CH_2Cl_2, 0 °C→RT (68%); f) $CuSO_4{\cdot}5H_2O$ (5 mol%), sodium ascorbate (10 mol%), *t*BuOH/H_2O, RT (86%); g) 2 M NaOH, dioxane/H_2O, 0 °C→RT (72%); h) H-Arg-AMC (**4**), DMF, EDC·HCl (1.1 equiv), DMAP (2 equiv), 0 °C→RT (68%); i) 2.6 M HCl in EtOAc, Et_2O, RT (87%).

mediated cycloaddition reaction. Therefore, Boc-protected propargylamine **31** was subjected to copper-catalyzed 1,3-dipolar cycloaddition with glycine derivatives **30**, using a mixture of sodium ascorbate and copper sulfate dissolved in water/*tert*-butanol, now resulting in the formation of Boc-Gly-[triazole]-Gly-OMe (**32**) in good yield (86%). Saponification of the methyl ester furnished Boc-Gly-[triazole]-Gly-OH (**33**), which was subsequently coupled to H-Arg-AMC (**4**) to furnish compound **34** in good yield (67%) after purification. Finally, Boc deprotection of compound **34** through treatment with hydrochloric acid in ethyl acetate gave H-Gly-[triazole]-Gly-Arg-AMC (**35**) in an excellent yield (87%).

Biological assays

Kinetic parameters of fluorogenic substrates

The thrombin generation method requires a substrate that is slowly hydrolyzed by thrombin to prevent substrate exhaustion before thrombin generation is complete, even at high substrate concentrations. Additionally, the binding constant (K_M) should be high for two reasons: Firstly, occupancy of the enzyme by substrate must be low to minimize any inhibition effects; as K_M represents the substrate concentration at which half of the enzyme is saturated, the substrate concentration must be below K_M. Secondly, the total amount of converted substrate must be minimal to exclude lower conversion rates due to declining substrate concentrations. These two requirements are met in a high K_M value. With respect to the aforementioned requirements, the ideal substrate is therefore highly specific for thrombin, has high K_M and low k_{cat}, and is vastly soluble and stable in plasma.

The amino acid composition determines the specificity of the substrate, and the complete chemical structure—including the leaving group—determines the kinetic constants of thrombin-mediated hydrolysis.[34,35] The relation between kinetic constants and chemical structure is predetermined, but cannot be predicted. To predict the behavior of a substrate in a thrombin generation (TG) experiment, the kinetic parameters K_M and k_{cat} must be determined. Inversely, from the desired behavior one can forecast some restraints on these kinetic constants. These restraints comprise the fraction of free thrombin as well as the rate and amount of fluorescent product formed (see Supporting Information). In practice, a useful substrate is water soluble, has $k_{cat} \geq 1\ s^{-1}$, $K_M \geq 200\ \mu M$, and can be used at a concentration of $\geq 200\ \mu M$. However, the higher the value of K_M the better, provided that k_{cat} also increases, maintaining the constraint $k_{cat} \geq K_M/[S]$ (for which [S] is the substrate concentration).

The rate of hydrolysis of the synthesized peptidyl-AMC compounds by thrombin (FIIa) was determined by monitoring the liberation of the 7-amino-4-methylcoumarin (AMC) fluorophore. The fluorescence increase was measured with a fluorimeter equipped with a 390/460 nm filter set (excitation/emission). To obtain a Michaelis–Menten plot, measurements were performed at various substrate concentrations and a fixed enzyme concentration. The kinetic parameters K_M and k_{cat} were obtained by determination of the initial reaction velocity (v_0) and subsequent fitting of the data to the Michaelis–Menten equation. The exact enzyme concentration was determined with a chromogenic assay that monitors the conversion of the chromogenic substrate S2238. Table 2 summarizes the data obtained.

In brief, the water-soluble substrate H-Gly-Gly-Arg-AMC (**2**) showed favorable kinetic parameters according to the described constraints for K_M, k_{cat}, and V_{max}. At both low and high substrate concentrations (Entries 2 and 3), this substrate fulfilled all the above-mentioned criteria: water soluble, $k_{cat} \geq 1\ s^{-1}$, and $K_M \geq 200\ \mu M$. In addition to H-Gly-Gly-Arg-AMC, the N-terminus-substituted derivatives (i.e., MeCO- (**6**), EtO_2C- (**8**), and CF_3CO- (**9**)) also demonstrated excellent kinetic parameters (Entries 4, 5, and 6). Substrate $EtSO_2$-Gly-Gly-Arg-AMC (**7**, Entry 7) required DMSO to be dissolved; however, it showed promising kinetic parameters ($K_M = 0.8$ mM and $k_{cat} = 1.51\ s^{-1}$). Conversely, the slightly larger aromatic substituents on the N-terminus (i.e., furyl (**11**) and pyridyl (**12**)) gave only moderate values for k_{cat} and K_M (Entries 8 and 9). Surprisingly, exchange of the amide bond between P_2 and P_3 in H-Gly-Gly-Arg-AMC for a triazole isostere resulted in complete loss of hydrolytic activity. In addition, the triazole moiety significantly affected the binding of this substrate in the active site of thrombin ($K_M = 0.77$ mM, Entry 10). As a control experiment H-Arg-AMC (compound **4**) was subjected to hydrolysis by thrombin. However, no signifi-

Table 2. Kinetic parameters for 15 peptidyl-AMC compounds on activated thrombin (FIIa) determined in BSA buffer at 37 °C.

Entry	Substrate	[S] [μM]	[E] [nM]	K_M [mM]	k_{cat} [s^{-1}]	V_{max} [$M^{-1}s^{-1}$]
1	Cbz-Gly-Gly-Arg-AMC·HCl[a,c] (**1**)	–	–	0.31	1.86	6.0×10^3
2	H-Gly-Gly-Arg-AMC·2 HCl (**2**)	300–2100	176	1.93	4.69	2.4×10^3
3	H-Gly-Gly-Arg-AMC·2 HCl (**2**)	200–1400	180	1.97	3.38	1.7×10^3
4	MeCO-Gly-Gly-Arg-AMC·HCl (**6**)	50–1000	88	2.38	1.38	579.8
5	EtO_2C-Gly-Gly-Arg-AMC·HCl (**8**)	50–1000	85	0.74	1.03	1.3×10^3
6	CF_3CO-Gly-Gly-Arg-AMC·HCl (**9**)	50–1000	79	2.62	1.89	721.4
7	$EtSO_2$-Gly-Gly-Arg-AMC·HCl[c] (**7**)	50–1000	84	0.80	1.51	538.8
8	Furyl-Gly-Gly-Arg-AMC·HCl[b] (**11**)	1000	100–400	0.17	0.20	1.2×10^3
9	Pyridyl-Gly-Gly-Arg-AMC·2 HCl[b] (**12**)	1000	100-400	0.06	0.12	3.3×10^3
10	H-Gly-[triazole]-Gly-Arg-AMC·2 HCl (**35**)	50–1000	86	0.77	0.09	116.8
11	H-Arg-AMC·2 HCl (**4**)	200–1400	191	_[d]	_[d]	_[d]
12	H-Ala-Arg-AMC·2 HCl (**14**)	50–1000	90	2.50	0.05	20.0
13	H-Ala-Pro-Arg-AMC·2 HCl (**18**)	50–1000	85	3.55	46.7	13×10^3
14	H-Ala-Val-Arg-AMC·2 HCl (**22**)	50–1000	108	9.48	5.10	538.0
15	H-Ala-Gly-Arg-AMC·2 HCl (**26**)	50–1000	87	2.33	2.14	918.5
16	Et-malonyl-Gly-Arg-AMC·HCl (**29**)	50–1000	87	1.66	6.99	4.2×10^3

[a] Kinetic data obtained from ref. [25]. [b] Kinetic parameters determined by varying [E] and fixed [S]. [c] Substrate dissolved in DMSO. [d] Not determined owing to insufficient substrate conversion.

cant amount of fluorescence was produced during this experiment. Extension of the Arg-AMC fragment with one amino acid, i.e., the dipeptidyl-AMC substrate H-Ala-Arg-AMC (**14**, Entry 12) also resulted in low fluorescence signal production ($k_{cat}=0.05\ s^{-1}$). Chain extension with one more amino acid, that is, structures with the general formula Ala-AA-Arg-AMC, greatly affected the kinetic parameters. Increasing the size of the second amino acid residue, going from glycine (**26**) to valine (**22**) or proline (**18**), resulted in a drastic change of both kinetic parameters (Entries 13–15). The proline-containing tripeptide **18** showed a very high k_{cat} value (46.7 s^{-1}), which was previously also shown for tripeptide H-Gly-Pro-Arg-AMC and its cyclic derivative;[36c] as a result, **18** cannot be used in TG experiments. Substrate **22** could be a suitable substrate for TG measurements, with both high K_M and k_{cat} (9.48 mM and 5.10 s^{-1}, respectively). Substrate H-Ala-Gly-Arg-AMC (**26**) has a binding constant of 2.33 mM and a rate of hydrolysis of 2.14 s^{-1} (Entry 13), making it ideal for TG measurements. Finally, SQ68 derivative Et-malonyl-Gly-Arg-AMC (**29**) also showed desirable kinetic parameters ($K_M=1.66$ mM and $k_{cat}=6.99\ s^{-1}$, Entry 14). These numbers deviate from the values found for SQ68 ($K_M=0.83$ mM and $k_{cat}=0.46\ s^{-1}$);[20a] they are, however, in accordance with data observed for DMMZ-Gly-Arg-*p*NA ($K_M=0.90$ mM and $k_{cat}=6.0\ s^{-1}$).[20b]

Substrates **2**, **6**–**9**, **22**, **26**, and **29** possess suitable K_M and k_{cat} values and were thus subsequently tested on serine protease factor Xa (FXa) to determine their kinetic parameters and thus thrombin specificity. Although the substrates H-Ala-Pro-Arg-AMC (**18**) and H-Gly-[triazole]-Gly-Arg-AMC (**35**) did not fulfill the thrombin substrate requirements, they were screened for FXa activity for comparison reasons. Conditions similar to those used for determining K_M and k_{cat} on thrombin were applied to determine the K_M and k_{cat} on FXa. The substrate concentration was varied between 50–1000 μM or 200–1400 μM, while a fixed enzyme concentration was used (ranging from 30 to 80 nM). The applied FXa enzyme concentration was lower than the FIIa concentration, as the presence of FXa in serum is 20-fold lower than FIIa on average (i.e., concentration FXa in plasma is 10 nM).[47] The exact FXa concentration was determined with a chromogenic assay that monitors the conversion of the chromogenic substrate MeO_2C-D-CHA-Gly-Arg-*p*NA (Pefachrome Xa). The obtained results are listed in Table 3.

A striking result was obtained for the substrate currently in use for thrombin generation testing (Cbz-Gly-Gly-Arg-AMC, **1**), which displayed only minor selectivity for FIIa over FXa (i.e., 0.31 mM over 0.71 mM, Entries 1, Tables 2 and 3, respectively). Gratifyingly, for the water-soluble derivative H-Gly-Gly-Arg-AMC (**2**), a high Michaelis constant ($K_M=13.14$ mM) was found, meaning poor FXa binding. This result indicated a ninefold selectivity toward FIIa over FXa for this substrate. Comparison of substrates **1** and **2** showed that substrate **1** has a far greater affinity for FXa than substrate **2** (19-fold higher). Next, substrates bearing either an acetyl or a trifluoroacetyl group at the N-terminus of Gly-Gly-Arg-AMC were screened for FXa activity. The acetyl-functionalized Gly-Gly-Arg-AMC (**6**) exhibited a high rate of hydrolysis (24.00 s^{-1}); however, the provided poor binding constant (11.0 mM) eliminates this compound as a suitable FXa substrate. The trifluoroacetyl-functionalized Gly-Gly-Arg-

Table 3. Kinetic parameters for 11 peptidyl-AMC compounds on serine protease factor Xa (FXa).

Entry	Substrate	[S] [μM]	[E] [nM]	K_M [mM]	k_{cat} [s^{-1}]	V_{max} [$M^{-1}s^{-1}$]
1	Cbz-Gly-Gly-Arg-AMC·HCl[a] (**1**)	200–1400	30	0.71	4.47	6.29×10^3
2	H-Gly-Gly-Arg-AMC·2 HCl (**2**)	200–1400	30	13.14	4.81	462.2
3	MeCO-Gly-Gly-Arg-AMC·HCl (**6**)	50–1000	73	11.0	24.00	2.81×10^3
4	CF_3CO-Gly-Gly-Arg-AMC·HCl (**9**)	50–1000	66	3.39	4.48	1.32×10^3
5	EtO_2C-Gly-Gly-Arg-AMC·HCl (**7**)	50–1000	80	6.50	1.05	161.5
6	$EtSO_2$-Gly-Gly-Arg-AMC·HCl[a] (**8**)	50–1000	80	1.96	0.53	272.3
7	H-Gly-[triazole]-Gly-Arg-AMC·2 HCl (**35**)	50–1000	80	_[a]	_[a]	_[a]
8	H-Ala-Pro-Arg-AMC·2 HCl (**18**)	50–1000	80	5.43	0.06	11.1
9	H-Ala-Val-Arg-AMC·2 HCl (**22**)	50–1000	80	_[b]	_[b]	_[b]
10	H-Ala-Gly-Arg-AMC·2 HCl (**26**)	50–1000	80	8.80	0.2	22.7
11	Et-malonyl-Gly-Arg-AMC·HCl (**29**)	50–1000	80	2.68	1.16	434.2

[a] Substrate dissolved in DMSO. [b] Not determined owing to insufficient substrate conversion.

AMC (**9**) was found to be a rather good FXa substrate, with a binding constant of 3.39 mM and a k_{cat} of 4.48 s^{-1} (Entry 4, Table 3). Both $EtSO_2$-Gly-Gly-Arg-AMC and EtO_2C-Gly-Gly-Arg-AMC (Entries 5 and 6) were found to be moderate FXa substrates and appeared to have a preference for the thrombin active site. No kinetic data could be obtained for H-Gly-[triazole]-Gly-Arg-AMC (**35**) and H-Ala-Val-Arg-AMC (**22**) as a result of insufficient substrate conversion (Entries 7 and 9). For the latter substrate (H-Ala-Val-Arg-AMC) this observation is remarkable, because a high rate of hydrolysis was found for thrombin (k_{cat} = 5.10 s^{-1}), which hence indicates the high thrombin specificity of this substrate. A similar effect was observed for H-Ala-Pro-Arg-AMC (**18**, Entry 8). The substrate was rapidly hydrolyzed by thrombin (k_{cat} = 46.7 s^{-1}); however, on FXa the turnover number was decreased to nearly zero (i.e., 0.06 s^{-1}). This effect can be attributed to the high specific binding of aliphatic amino acids in the S_2 binding site of thrombin, while FXa has a preference for aromatic amino acids at P_2 (e.g., phenylalanine or tryptophan).[35] The substrate Ala-Gly-Arg-AMC (**26**) emerged as a thrombin-selective substrate, as both the FXa binding and turnover numbers are low (8.80 mM and 0.2 s^{-1}, respectively, Entry 10). Finally, the affinity of Et-malonyl-Gly-Arg-AMC (**29**) was slightly higher for FIIa than for FXa (1.66 and 2.68 mM, respectively); however, the rate of hydrolysis was significantly in favor of thrombin (6.99 s^{-1} for FIIa compared to 1.16 s^{-1} for FXa). These results indicate that substrates **7**, **22**, and **26** are particularly suitable substrates for thrombin generation testing, while substrates **2**, **8**, and **29** can also be considered potential suitable candidates. These promising substrates will be further evaluated on their applicability in calibrated automated thrombography.

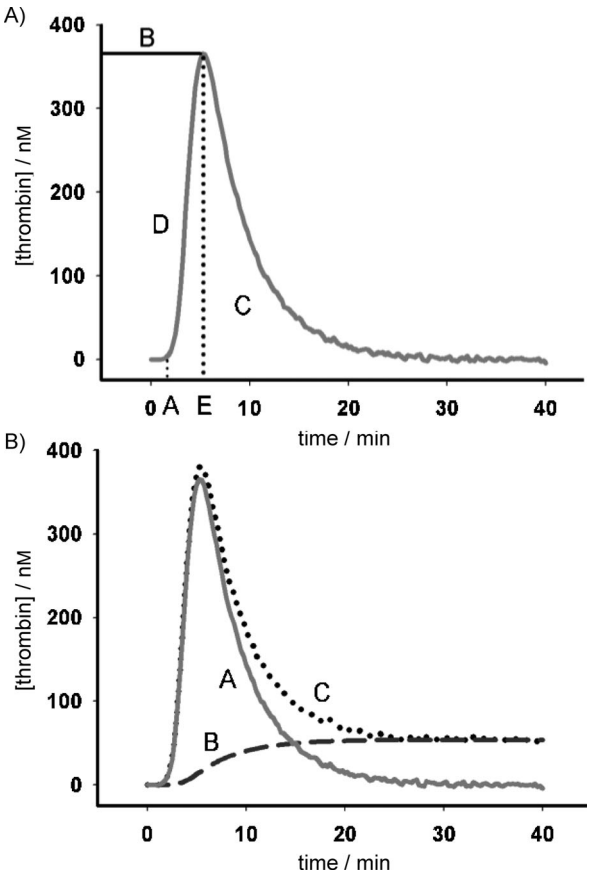

Figure 3. A) Parameters of the thrombogram. A: lag time (min); B: peak height (nM); C: endogenous thrombin potential (ETP = area under the curve [nM × min]); D: slope (V_{max} [nM min^{-1}]); E: time-to-peak (ttP), which provides information about the total length of the procoagulant phase (i.e., initiation, amplification, and propagation, together).[53] B) Thrombin-time integral (curve C) is a composite of α_2M-thrombin-time integral (curve B) and the free thrombin-time integral (curve A).[54]

Fluorogenic substrates in continuous thrombin generation

Calibrated automated thrombography (CAT) has been applied for the determination of a wide variety of haemostatic defects such as hyper- and hypocoagulability,[48] bleeding tendencies,[49] and von Willebrand disease.[50] In addition, the use of CAT allows screening and testing of new antithrombotics.[51] However, reports describing the use of CAT for the screening of fluorogenic peptides suitable for thrombin generation testing are extremely limited. One of the few examples was reported by Ramjee, who used a small series of fluorogenic peptides to monitor the effect on TG.[24] The substrates used were not slow-reacting substrates and thus not suitable for TG testing.

The general form of a thrombin generation curve (TGC or thrombogram) is shown in Figure 3 A. At the start of the coagulation only minute quantities of thrombin are present. This lag phase, also called the initiation phase,[9] is followed by an explosive rise in thrombin concentration (production phase). The time required for the offset of extensive thrombin formation is known as the lag time. Because clot formation starts with the increase in thrombin concentration—the end of the lag time—the clotting time roughly equals the lag time (A in Figure 3 A). The slope of the TGC equals the maximum velocity (V_{max}) of thrombin formation during the production phase. The point at which the velocity of thrombin formation equals the velocity of thrombin decay (i.e., peak maximum) is known as the peak height (B in Figure 3 A). The final phase is the inactivation phase;[9] here the antithrombin activity gains over prothrombin conversion, which gives rise to a decline in the amount of thrombin. The thrombogram thus provides specific parameters to describe the complete thrombin generation profile, correlated with the various stages of coagulation. The three most important parameters are the lag time, peak height, and the area under the curve or endogenous thrombin potential (ETP),[52] which represents the amount of enzymatic work that can be performed by thrombin during its lifetime (C in Figure 3 A). The ETP is derived from the term thrombin potential (TP) introduced by Hemker et al.[20a] to more accurately describe the overall effect of thrombin on clotting systems.

To correctly construct a TGC (time versus thrombin concentration) a series of mathematical operations on the raw data is required. The first step entails the transformation of the velocity of fluorescence change (d*F*/d*t*) into a thrombin concentration. The resulting curve requires correction for factors such as substrate consumption and the inner-filter effect (nonlinearity of fluorescence intensity with increasing concentration).[55] The velocity of fluorescence increase per unit enzyme therefore de-

creases during the experiment as a function of the amount of substrate converted by the enzyme. Because the fluorescence increase is not linear with thrombin concentration, a method is required to correct for this effect. To this end, each TG experiment was accompanied by an experiment in which a fixed amount of thrombin activity (in the form of α_2-macroglobulin–thrombin complex) was active, so that at every substrate and product concentration the appropriate calibration factor could be read and applied. Next, the first derivative of the corrected fluorescence progress curve gives the correct thrombin generation curve (i.e., curve C, Figure 3B). Two molecular species with amidolytic activity contribute to the shape of this curve. The first is free thrombin (curve A, Figure 3B) and the second is thrombin bound to α_2-macroglobulin (α_2M-T; curve B, Figure 3B). The latter arises from the fact that thrombin, when bound to α_2M, although completely devoid of any known biological activity, retains its capacity to hydrolyze small substrates. Through mathematical processing α_2M-T activity can be calculated and subtracted from the composite curve C (described by Hemker et al.).[20a,52] The obtained free-thrombin curve (curve A, Figure 3B) is then fitted to the first derivative of the so-called W-function to find the appropriate thrombin concentration. The essence of this fit procedure is described by Wagenvoord et al.[56] This final transformation then results in thrombin generation curve A, from which the aforementioned parameters can be deduced.

Continuous automated calibrated thrombin generation experiments were initially performed using the water-soluble tripeptide H-Gly-Gly-Arg-AMC·2HCl (**2**). Based on the kinetic parameter screening this substrate was expected to be a suitable substrate for TG testing. Thrombin generation was measured according to the protocol described by Hemker and co-workers.[25] As shown in Figure 4A, a normal thrombogram was obtained for water-soluble tripeptide **2**. Comparison of the imperative thrombogram parameters of this compound and the Cbz-protected substrate **1** showed considerable differences. Besides a significantly shorter lag time, a lower peak height (FIIa max) and ETP value were observed (see Table 4). Because high substrate concentrations cause less thrombin to be available for binding of its natural substrate and for interaction with antithrombins,[57] this is reflected in the shape and size of the thrombogram and thus the amount of thrombin. This led us to investigate the effect of various concentrations of the substrate H-Gly-Gly-Arg-AMC (**2**) on thrombin generation (Figure 4B).

With an increasing concentration of fluorogenic substrate (200–1200 μM), an increase in the peak heights of the thrombograms was observed. With increased peak height, an increase in ETP was also observed. A plot of the ETP against substrate concentration (insert Figure 4B) shows an approximately linear relationship with an intercept at the ordinate (i.e., [S] = 0) corresponding to an ETP value of ~1000 nM min, identical to the

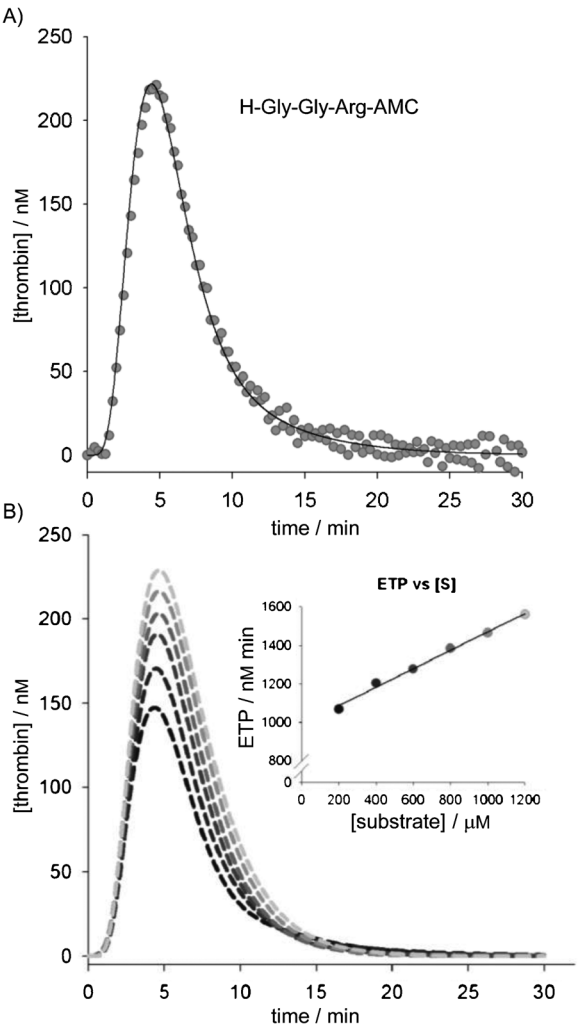

Figure 4. A) Thrombin generation curve for H-Gly-Gly-Arg-AMC (1000 μM) in normal platelet-poor plasma. Grey dots represent the derivative of the measured progress curve after correction for α_2M-T activity. The black line is the calculated free thrombin curve using the constants obtained from the calibration curve (not shown). B) Thrombin generation at various substrate concentrations, from light- to dark-grey: 1200, 1000, 800, 600, 400, and 200 μM H-Gly-Gly-Arg-AMC (**2**); insert: ETP versus substrate concentration.

Table 4. Parameters acquired from the thrombograms obtained via CAT.[a]

Entry	Substrate	Lag time [min]	Peak [nM]	ttPeak [min][b]	ETP [nM min]
1	Cbz-Gly-Gly-Arg-AMC·HCl[c] (**1**)	3.10 ± 1.40	458 ± 60	ND	1879 ± 284
2	H-Gly-Gly-Arg-AMC·2HCl (**2**)	1.56 ± 0.13	211.6 ± 11.9	4.71 ± 0.20	1409.6 ± 79.5
3	CH_3CO-Gly-Gly-Arg-AMC·HCl (**6**)	2.32 ± 0.11	188.2 ± 7.8	5.89 ± 0.13	1360.3 ± 47.2
4	CF_3CO-Gly-Gly-Arg-AMC·HCl (**9**)	2.76 ± 0.31	223.4 ± 4.1	6.27 ± 0.31	1566.5 ± 47.0
5	EtO_2C-Gly-Gly-Arg-AMC·HCl (**7**)	2.56 ± 0.11	369.6 ± 4.9	5.19 ± 0.11	2548.0 ± 80.5
6	$EtSO_2$-Gly-Gly-Arg-AMC·HCl (**8**)	2.50 ± 0.01	226.4 ± 3.1	5.44 ± 0.11	1587.5 ± 26.7
7	H-Ala-Gly-Arg-AMC·2HCl (**26**)	2.44 ± 0.11	251.9 ± 3.3	5.12 ± 0.12	1487.8 ± 44.4
8	H-Ala-Val-Arg-AMC·2HCl (**22**)	2.25 ± 0.18	226.6 ± 3.6	4.50 ± 0.18	1288.0 ± 21.9
9	Et-malonyl-Gly-Arg-AMC·HCl (**29**)	2.50 ± 0.18	377.2 ± 14.3	5.31 ± 0.21	2024.0 ± 48.5

[a] Experiments performed in quadruplicate. [b] ttPeak: time-to-peak; ND: not determined. [c] Data obtained from ref. [59].

standard (normal) value.[20a] The influence of substrate concentration on ETP becomes negligible when the amount of free thrombin (T_{free}) is calculated by correcting for the substrate concentration [S] and substrate binding constant K_M [Eq. (1)]:[25]

$$T_{free} = [T_{tot}] \times K_M/(K_M + [S]) \quad (1)$$

From the preliminary screening of kinetic parameters on FIIa and FXa we selected seven other substrates for continuous thrombin generation assessment. The thrombograms were measured in normal platelet-poor plasma with a final substrate concentration in the well of 1000 μM according to the procedure described below in the Experimental Section. Thrombin generation was monitored for 40 min, after which the raw data were processed, resulting in the thrombograms of which a selection is depicted in Figure 5. The obtained thrombograms show only minute deviations in shape with respect to the thrombogram obtained in platelet-poor plasma using the substrate Cbz-Gly-Gly-Arg-AMC (**1**). This accounts for all the eight substrates tested. In the case of Et-malonyl-Gly-Arg-AMC some random scattering was observed at the end of the experiment, and therefore only 30 min are displayed.

The W-function fit procedure was applied to all the thrombograms in order to appropriately determine the main parameters related to the measured substrates (data summarized in Table 4). For all the substrates a normal lag time (2.25–2.82 min) and time-to-peak (4.50–6.27 min) were observed, suggesting that the clotting system does not suffer any inhibitory effects caused by the substrates. The decreased lag time observed for H-Gly-Gly-Arg-AMC (see above) can be caused by clotting factor activation. Supplementary research is required to investigate this phenomenon. Peak heights for $EtCO_2$-Gly-Gly-Arg-AMC (**7**) and Et-malonyl-Gly-Arg-AMC (**29**) are rather high as a result of the equally high ETP values found for these substrates.[58] The remaining substrates all showed appropriately high ETP values relative to ETP in plasma (1000 nM min). On average, a slight decrease of the ETP, lag time, and peak height values for the tested substrates was observed in comparison with the values obtained for Cbz-Gly-Gly-Arg-AMC (Table 4, Entry 1).

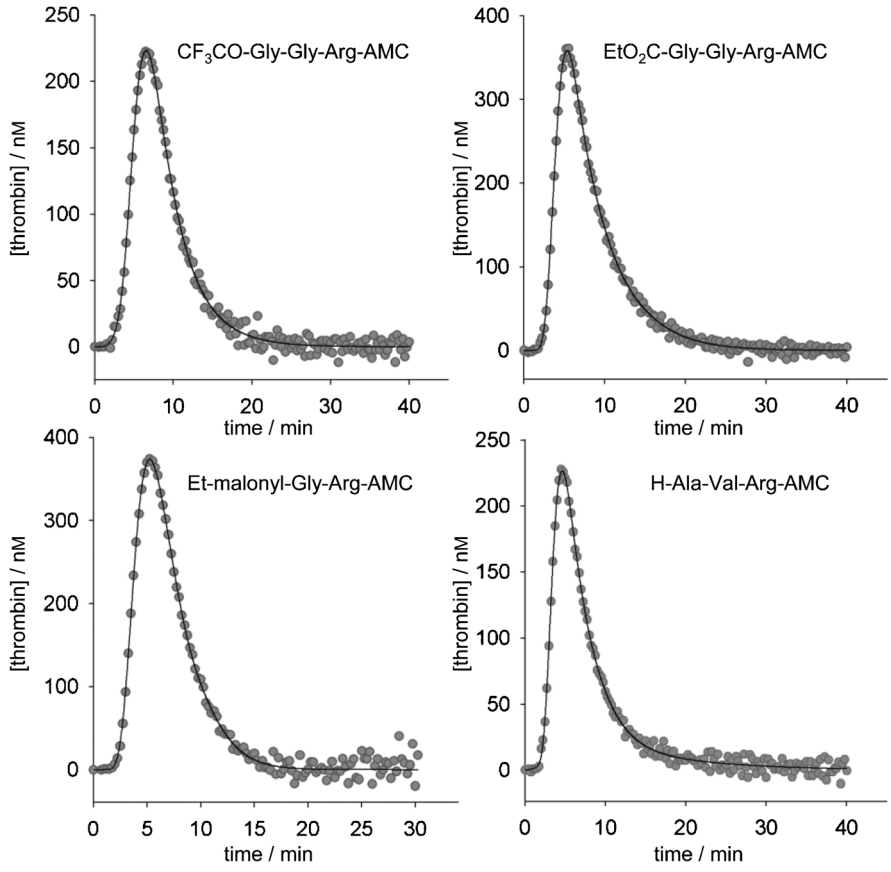

Figure 5. Selection of thrombograms obtained after thrombin generation measurement in normal platelet-poor plasma at 37 °C over 40 min using a substrate concentration of 1000 μM. The parameters obtained from the thrombin generation curves are listed in Table 4.

Conclusions

A series of 13 arginine–AMC-containing peptides were successfully synthesized by starting from key intermediate H-Arg-AMC. The water-soluble variant, H-Gly-Gly-Arg-AMC·2 HCl, was produced in a straightforward four-step protocol and served as the basis for further optimization by N-terminal substitution. A small library of peptides was constructed in reasonable to good yields, starting from H-Gly-Gly-Arg-AMC using either strong electrophiles (RSO_2Cl, RCOCl or ROCOCl) or carboxylates in combination with peptide coupling methods. Additionally, several peptides with small structural changes in the amino acid sequence (i.e., P_2 and P_3) were synthesized in good overall yields. An efficient three-step protocol was applied to the synthesis of an SQ68 mimic, Et-malonyl-Gly-Arg-AMC, resulting in the target compound in an overall yield of 32%. The introduction of a triazole moiety, replacing an amide bond, proceeded smoothly by applying the copper-catalyzed 1,3-dipolar cycloaddition reaction on Boc-protected propargylamine and methyl 2-azidoacetate, finally leading to the triazole-containing tripeptide H-Gly-[triazole]-Gly-Arg-AMC in good overall yield. The aforementioned fluorogenic peptide substrates were subsequently subjected to a biological evaluation. Considering the primary criteria providing suitable substrates for thrombin generation testing (i.e., appropriate kinetic parameters on FIIa,

FIIa selectivity over FXa, and water solubility), screening of the 13 fluorogenic substrates resulted in the selection of five highly suitable substrates. These substrates, H-Gly-Gly-Arg-AMC, $EtCO_2$-Gly-Gly-Arg-AMC, H-Ala-Gly-Arg-AMC, H-Ala-Val-Arg-AMC, and Et-malonyl-Gly-Arg-AMC provided excellent kinetic constants K_M and k_{cat} for thrombin and displayed high selectivity for thrombin over factor Xa. In addition, good solubility in physiological media (water, buffer, and plasma) was observed for all these substrates. Subsequent thrombin generation measurements, performed in PPP, was conducted on a series of eight fluorogenic substrates displaying proper thrombin generation curves for most of these substrates; moreover, the main parameters obtained from the thrombograms (i.e., lag time, time-to-peak, and ETP) were similar to the values reported for Cbz-Gly-Gly-Arg-AMC. Slight deviation was found for H-Gly-Gly-Arg-AMC (short lag time) and the substrates Et-malonyl-Gly-Arg-AMC and $EtCO_2$-Gly-Gly-Arg-AMC (higher ETP). However, Cbz-Gly-Gly-Arg-AMC has proven not to be the most suitable substrate for TGT, thus leaving considerable room for redefining standard thrombogram parameter values. The outstanding kinetic parameters, high solubility, and formation of well-defined thrombin generation curves of the five above-mentioned substrates make them highly appropriate compounds for the replacement of the substrate in current use. Moreover, based on the set criteria and the obtained results we recommend the replacement of Cbz-Gly-Gly-Arg-AMC with H-Ala-Val-Arg-AMC as the most suitable substrate. Currently, a more detailed investigation of the behavior of the selected substrates on other clotting factors, as well as in platelet-rich plasma, is being conducted in our laboratories. Moreover, the suitability of the substrates presented herein is further assessed by a new mathematical procedure, the so-called H-transform.[60] This method allows rapid definition of the applicable concentration range for a specific substrate in thrombin generation; the results will be presented in a forthcoming report. Furthermore, we will focus on the application of these substrates in microfluidic devices,[36b] which allow rapid diagnosis of blood or plasma samples and thus can be applied in so-called point-of-care tests (POCT).

Experimental Section

Synthesis

See the Supporting Information for detailed synthetic procedures of tripeptides **2**, **6**–**9**, **11**, **12**, **14**, **18**, **22**, **26**, **29**, and **35**.

Biological assays

Sample preparation

Substrate preparation: A mixture of a fluorogenic substrate and $CaCl_2$ (denoted FluCa) was prepared for each thrombin generation experiment as follows: to 875 μL BSA5 buffer at 37 °C, $CaCl_2$ (100 μL, 1 M) and a solution of the fluorogenic substrate (25 μL, 100 mM in BSA buffer ($BSA60^+$)) were added and immediately mixed vigorously. All substrates were dissolved in BSA buffer with the exception of Cbz-Gly-Gly-Arg-AMC and $EtSO_2$-Gly-Gly-Arg-AMC, which were dissolved in DMSO.

Trigger (rTF): Trigger solution for the extrinsic system was composed of 300 pM recombinant tissue factor (rTF) in HEPES buffer.

Calibrator (α_2M-T): To obtain stable thrombin-like activity in plasma, α_2-macroglobulin–thrombin complex (α_2M-T) was used, prepared as described previously by Hemker et al.[25]

Blood and plasma: Blood was obtained through antecubital venipuncture (1 volume trisodium citrate (0.13 M) to 9 volumes blood) from healthy consenting individuals. Free-flow or minimal suction was employed; vacuum containers were avoided. Platelet-rich plasma (PRP) was collected from the upper 3/4 volume of plasma supernatant after centrifugation at 265 *g* for 10 min at room temperature. The platelets were counted (Beckman Coulter counter), and PRP was adjusted to 150×109 platelets L^{-1} with its own platelet-poor plasma (PPP). PRP was always used within 1 h after venipuncture. PPP was prepared by centrifuging twice at 2900 *g* for 10 min at room temperature. To avoid contamination with procoagulant microparticles from aging platelets, PPP was prepared within 30 min after venipuncture.

Determination kinetic parameters

Typically 0.025 mmol fluorogenic substrate was dissolved in 0.25 mL BSA buffer ($BSA60^+$) to give a 100 mM stock solution. From this stock solution a series of dilutions was prepared to give final substrate concentrations of 0, 50, 100, 200, 400, 600, 800, and 1000 μM in the well. A thrombin (FIIa) solution of 0.6 μM was prepared from a 4.5 μM FIIa stock solution by dilution with BSA buffer (BSA5). To four wells of a round-bottom 96-well plate, 100 μL of each appropriate substrate concentration was added. The plate was placed in an Ascent fluorimeter equipped with a 390/460 nm filter set (excitation/emission) and allowed to warm to 37 °C (~5 min). Enzyme solution (20 μL, 0.6 μM) was added to each well (100 nM FIIa end concentration in wells; 8×4 wells in total) to initiate hydrolysis. In a typical experiment, fluorescence was measured over 40 min at 37 °C. The obtained data were organized in Microsoft Excel, and the kinetic parameters were obtained by fitting the data to the Michaelis–Menten equation. For the determination of K_M and k_{cat}, the initial reaction velocity of the first 10 min was used. The amidolytic activity was calculated by comparing the arbitrary fluorescence values to those of a calibration curve.

Determination exact enzyme concentration

The exact enzyme concentration was determined by monitoring the conversion of a chromogenic substrate using a microplate reader (EL808, Bio-Tek Instruments Inc., Burlington, VT, USA) measuring the absorption at 405 nm. The substrate used for FIIa and α_2M-T activity measurements was S2238 (600 μM in 175 mM NaCl, 50 mM Tris·HCl, pH 7.9) and for FXa the substrate used was Pefachrome Xa (510 μM in 175 mM NaCl, 0.02% NaN_3, 3.0 μM α-NAPAP, 50 mM Tris·HCl, pH 7.9).

For the determination of the exact enzyme concentration (FIIa, α_2M-T or FXa) the enzyme stock solution (used during the kinetic experiments) was diluted with ovalbumin buffer (BOA) to obtain a final concentration of 1.2 nM for FIIa and α_2M-T, and 0.8 nM for FXa. Subsequently, four wells of a microtiter plate were filled with 100 μL diluted enzyme solution, after which the plate was warmed to 37 °C for 5–10 min. To each of the wells was added 20 μL substrate (see above) using a multi-pipette. The microtiter plate was placed in a microplate reader set at 37 °C, and the conversion of substrate was monitored for 5 min. The enzyme activity determina-

tions were performed in triplicate or quadruplicate. Finally, the enzyme concentration was calculated using dedicated software.

Keywords: ETP · fluorogenic substrates · peptide synthesis · thrombin · thrombograms

Fluorescence-based measurement of thrombin activity

A detailed experimental description of calibrated automated thrombin generation measurements can be found in references [25] and [61]. The development of fluorescence intensity from 7-amino-4-methylcoumarin (AMC) was typically measured in a 96-well plate fluorimeter (Ascent reader, Thermolabsystems OY, Helsinki, Finland) equipped with a 390/460 nm filter set (excitation/emission) and a dispenser. Immulon 2HB, round-bottom 96-well plates (Dynex) were used. Minimal four readings were performed per minute, and experiments were carried out in quadruplicate unless otherwise indicated. In a typical thrombin generation experiment using CAT, each thrombin generation sample (TG well) was compared with a fixed amount of constant thrombin activity which was added to a parallel sample of the same plasma, that is, calibrator (CL well). From the resulting curve, the calibration factor at any level of fluorescence could be determined, and the exact thrombin concentration in the sample in which TG was occurring could thus be calculated.

To each well, 80 μL NPPP was added. Wells in which TG was measured received 20 μL buffer containing the trigger but without Ca^{2+}. Wells in which constant thrombin-like activity was to be measured received 20 μL of the α_2M-T solution at the required concentration as indicated. For NPPP, the trigger consisted of 30 pM rTF and 24 μM phosphatidylserine/phosphatidylcholine/phosphatidylethanolamine vesicles in HEPES-buffered saline. For PRP, the trigger was 20 μL 3 pM rTF without additional PL.

The 96-well plate was placed in the fluorimeter and allowed to warm to 37 °C (at least 10 min). The dispenser of the fluorimeter was flushed with warm 100 mM $CaCl_2$ solution, emptied, and then flushed with warm FluCa. At the start of the experiment, the instrument dispensed 20 μL FluCa into all wells to be measured, which was registered as $t=0$, after shaking for 10 s, and fluorescence reading was started. The experiment was halted after 40 min, and the obtained data were exported to an appropriate software program for further processing.

Data handling

The raw data of optical density measurements were processed with KC Junior microplate data analysis software. Fluorescence measurements of thrombin activity were exported to SigmaPlot version 9.0 (Systat Software Inc., Point Richmond, CA, USA) or to Microsoft Excel (2002 or higher) for further mathematical processing.

Acknowledgements

The authors thank Dr. R. H. Blaauw (Chiralix BV, Nijmegen, NL), Dr. D. T. S. Rijkers (University of Utrecht, Utrecht, NL), Dr. P. J. L. M. Quaedflieg (DSM, Geleen, NL), and P. J. H. M. Adams (Radboud University Nijmegen) for useful synthetic suggestions and discussions. Dr. R. Al Dieri and Dr. E. de Smedt (Synapse BV) are kindly acknowledged for technical biochemical support and fruitful discussions. These investigations were supported with financial aid from the Netherlands Technology Foundation (STW).

[1] M. J. Costanzo, H. R. Almond, Jr., L. R. Hecker, M. R. Schott, S. C. Yabut, H.-C. Zhang, P. Andrade-Gordon, T. W. Corcoran, E. C. Giardino, J. A. Kauffman, J. M. Lewis, L. de Garavilla, B. J. Haertlein, B. E. Maryanoff, *J. Med. Chem.* **2005**, *48*, 1984 – 2008.
[2] D. J. Angiolillo, P. Capranzano, *Am. Heart J.* **2008**, *156*, 10S – 15S.
[3] A. T. Askari, A. W. Messerli, A. M. Lincoff, *Management Strategies in Antithrombotic Therapy*, Wiley, Chichester, **2007**.
[4] W. Bode, I. Mayr, U. Baumann, R. Huber, S. R. Stone, J. Hofsteenge, *EMBO J.* **1989**, *8*, 3467 – 3475.
[5] a) A. Schwienhorst, *Cell. Mol. Life Sci.* **2006**, *63*, 2773 – 2791; b) P. C. A. Kam, N. Kaur, C. L. Thong, *Anaesthesia* **2005**, *60*, 565 – 574; c) L.-A. Linkins, J. I. Weitz, *Curr. Pharm. Des.* **2005**, *11*, 3877 – 3884.
[6] For reviews on thrombin inhibitors, see: a) J. Das, S. D. Kimball, *Bioorg. Med. Chem.* **1995**, *3*, 999 – 1007; b) K. Menear, *Expert Opin. Invest. Drugs* **1999**, *8*, 1373 – 1384; c) C. A. Kontogiorgis, D. Hadjipavlou-Litina, *Curr. Med. Chem.* **2003**, *10*, 525 – 577; d) C. Becattini, A. Lignani, G. Agnelli, *Drug Des. Devel. Ther.* **2010**, *4*, 49 – 60.
[7] A. Tripodi, P. M. Mannucci, *Clin. Chem.* **1984**, *30*, 1392 – 1395.
[8] D. A. Triplett, *Clin. Chem.* **2000**, *46*, 1260 – 1269.
[9] K. G. Mann, K. Brummel, S. Butenas, *J. Thromb. Haemostasis* **2003**, *1*, 1504 – 1514.
[10] N. Salooja, D. J. Perry, *Blood Coagulation Fibrinolysis* **2001**, *12*, 327 – 337.
[11] J. L. Francis, *Platelets* (Ed.: A. D. Michelson), Academic Press, San Diego, **2002**, pp. 325 – 335.
[12] T. W. Barrowcliffe, M. Cattaneo, G. M. Podda, P. Bucciarelli, F. Lussana, A. Lecchi, C. H. Toh, H. C. Hemker, S. Béguin, J. Ingerslev, B. Sørensen, *Haemophilia* **2006**, *12*, 76 – 81.
[13] G. T. Gerotziafas, F. Depasse, J. Busson, L. Leflem, I. Elalamy, M. M. Samama, *Thromb. J.* **2005**, *3*, 16 – 26.
[14] A. Beilfu, M. Grandoch, F. Wenzel, T. Hohlfeld, K. Schrör, A.-A. Weber, *Ther. Drug Monit.* **2008**, *30*, 740 – 743.
[15] H. C. Hemker, R. Al Dieri, E. de Smedt, S. Béguin, *Thromb. Haemostasis* **2006**, *96*, 553 – 561.
[16] R. G. Macfarlane, R. Biggs, *J. Clin. Pathol.* **1953**, *6*, 3 – 8.
[17] W. R. Pitney, J. V. Dacie, *J. Clin. Pathol.* **1953**, *6*, 9 – 14.
[18] H. C. Hemker, G. M. Willems, S. Béguin, *Thromb. Haemostasis* **1986**, *56*, 9 – 17.
[19] a) For the development of thrombin-specific, chromogenic peptide substrates, see the pioneering work by: L. Svendsen, B. Blomback, M. Blomback, P. I. Olsson, *Thromb. Res.* **1972**, *1*, 267 – 278; b) L. G. Svendsen, J. Fareed, J. M. Walenga, D. Hoppensteadt, *Semin. Thromb. Hemostasis* **1983**, *9*, 250 – 262.
[20] a) H. C. Hemker, S. Wielders, H. Kessels, S. Béguin, *Thromb. Haemostasis* **1993**, *70*, 617 – 624; b) D. T. S. Rijkers, S. J. H. Wielders, G. I. Tesser, H. C. Hemker, *Thromb. Res.* **1995**, *79*, 491 – 499.
[21] S. Langlet, G. Quentin, G. Contant, J. C. Ghnassia, *Ann. Biol. Clin.* **1999**, *57*, 191 – 196.
[22] K. Vanschoonbeek, M. A. H. Feijge, R. J. W. van Kampen, H. Kenis, H. C. Hemker, P. L. A. Giesen, J. W. M. Heemskerk, *J. Thromb. Haemostasis* **2004**, *2*, 476 – 484.
[23] H. C. Hemker, P. L. Giesen, M. Ramjee, R. Wagenvoord, S. Béguin, *Thromb. Haemostasis* **2000**, *83*, 589 – 591.
[24] M. K. Ramjee, *Anal. Biochem.* **2000**, *277*, 11 – 18.
[25] H. C. Hemker, P. Giesen, R. Al Dieri, V. Regnault, E. de Smedt, R. Wagenvoord, T. Lecompte, S. Béguin, *Pathophysiol. Haemostasis Thromb.* **2003**, *33*, 4 – 15.
[26] M. Zimmerman, B. Ashe, E. C. Yurewicz, G. Patel, *Anal. Biochem.* **1977**, *78*, 47 – 51.
[27] Y. Kanaoka, T. Takahashi, H. Nakayama, *Chem. Pharm. Bull.* **1977**, *25*, 3126 – 3128.
[28] T. Kato, T. Hama, K. Kojima, T. Nagatsu, S. Sakakibara, *Clin. Chem.* **1978**, *24*, 1163 – 1166.
[29] S. Kunugi, M. Fukuda, R. Hayashi, *Eur. J. Biochem.* **1985**, *153*, 37 – 40.
[30] T. Morita, H. Kato, S. Iwanaga, K. Takada, T. Kimura, S. Sakakibara, *J. Biochem.* **1977**, *82*, 1495 – 1498.

[31] S. Kawabatal, T. Miura, T. Morita, H. Kato, K. Fujikawa, S. Iwanaga, K. Takada, T. Kimura, S. Sakakibara, *Eur. J. Biochem.* **1988**, *172*, 17 – 25.
[32] Y. Ohno, H. Kato, T. Morita, S. Iwanaga, K. Takada, S. Sakakibara, J. Stenflo, *J. Biochem.* **1981**, *90*, 1387 – 1395.
[33] H. Kato, N. Adachi, Y. Ohno, S. Iwanaga, K. Takada, S. Sakakibara, *J. Biochem.* **1980**, *88*, 183 – 190.
[34] B. J. Backes, J. L. Harris, F. Leonetti, C. S. Craik, J. A. Ellman, *Nat. Biotechnol.* **2000**, *18*, 187 – 193.
[35] S. T. Furlong, R. C. Mauger, A. M. Strimpler, Y.-P. Liu, F. X. Morris, P. D. Edwards, *Bioorg. Med. Chem.* **2002**, *10*, 3637 – 3647.
[36] a) A. J. Dirks, S. S. van Berkel, H. I. V. Amatdjais-Groenen, F. L. van Delft, F. P. J. T. Rutjes, J. J. L. M. Cornelissen, R. J. M. Nolte, *Soft Matter* **2009**, *5*, 1692 – 1704; b) K. Koch, S. S. van Berkel, M. M. E. B. van de Wal, P. J. Nieuwland, J. C. M. van Hest, F. P. J. T. Rutjes, *J. Appl. Phys.* **2009**, *105*, 102012/1 – 102012/5; c) S. S. van Berkel, B. van der Lee, F. L. van Delft, F. P. J. T. Rutjes, *Chem. Commun.* **2009**, 4272 – 4274.
[37] Available from Bachem AG, Switzerland, I-1140, Cat. no. 102601-58-1.
[38] a) F. Jean, A. Boudreault, A. Basak, N. G. Seidah, C. Lazure, *J. Biol. Chem.* **1995**, *270*, 19225 – 19231; b) P. D. Edwards, R. C. Mauger, K. M. Cottrell, F. X. Morris, K. K. Pine, M. A. Sylvester, C. W. Scott, S. T. Furlong, *Bioorg. Med. Chem. Lett.* **2000**, *10*, 2291 – 2294; c) D. J. Maly, F. Leonetti, B. J. Backes, D. S. Dauber, J. L. Harris, C. S. Craik, J. A. Ellman, *J. Org. Chem.* **2002**, *67*, 910 – 915.
[39] D. T. S. Rijkers, H. P. H. M. Adams, H. C. Hemker, G. I. Tesser, *Tetrahedron* **1995**, *51*, 11235 – 11250.
[40] An elegant enzymatic approach was recently published: T. Nuijens, C. Cusan, J. A. W. Kruijtzer, D. T. S. Rijkers, R. M. J. Liskamp, P. J. L. M. Quaedflieg, *J. Org. Chem.* **2009**, *74*, 5145 – 5150.
[41] For an overview of coupling methods, see: S.-Y. Han, Y.-A. Kim, *Tetrahedron* **2004**, *60*, 2447 – 2467.
[42] G. Freyburger, M. Dubreuil, A. Audebert, S. Labrouche, J. C. Pistre, I. Molinari, F. Dubecq, C. Laville, X. Villanove, *Haemostasis* **2001**, *31*, 32 – 41.
[43] For a review, see: a) Y. L. Angell, K. Burgess, *Chem. Soc. Rev.* **2007**, *36*, 1674 – 1689. Selected publications: b) W. S. Horne, C. D. Stout, M. R. Ghadiri, *J. Am. Chem. Soc.* **2003**, *125*, 9372 – 9376; c) W. S. Horne, M. K. Yadav, C. D. Stout, M. R. Ghadiri, *J. Am. Chem. Soc.* **2004**, *126*, 15366 – 15367; d) V. D. Bock, D. Speijer, H. Hiemstra, J. H. van Maarseveen, *Org. Biomol. Chem.* **2007**, *5*, 971 – 975.
[44] For examples of biologically active triazoles, see: a) R. Alvarez, S. Velazquez, F. San, S. Aquaro, C. De, C. F. Perno, A. Karlsson, J. Balzarini, M. Camarasa, *J. Med. Chem.* **1994**, *37*, 4185 – 4191; b) J. S. Tullis, J. C. Van-Rens, M. G. Natchus, M. P. Clark, B. De, L. C. Hsieh, M. J. Janusz, *Bioorg. Med. Chem. Lett.* **2003**, *13*, 1665 – 1668; c) C. W. Tornøe, S. J. Sanderson, J. C. Mottram, G. H. Coombs, M. Meldal, *J. Comb. Chem.* **2004**, *6*, 312 – 324; d) D.-K. Kim, J. Kim, H.-J. Park, *Bioorg. Med. Chem. Lett.* **2004**, *14*, 2401 – 2405; e) A. Brik, J. Alexandratos, Y.-C. Lin, J. H. Elder, A. J. Olson, A. Wlodawer, D. S. Goodsell, C.-H. Wong, *ChemBioChem* **2005**, *6*, 1167 – 1169.
[45] a) C. W. Tornøe, C. Christensen, M. Meldal, *J. Org. Chem.* **2002**, *67*, 3057 – 3064; b) V. V. Rostovtsev, L. G. Green, V. V. Fokin, K. B. Sharpless, *Angew. Chem.* **2002**, *114*, 2708 – 2711; *Angew. Chem. Int. Ed.* **2002**, *41*, 2596 – 2599.
[46] P. L. Golas, K. Matyjaszewski, *QSAR Comb. Sci.* **2007**, *26*, 1116 – 1134.
[47] H. C. Hemker, "The Mode of Action of Heparin in Plasma" in *Thrombosis and Haemostasis* (Eds.: M. Verstraete, J. Vermylen, R. Lijnen, J. Arnout), Leuven University Press, Leuven, **1987**, pp. 17 – 36.
[48] a) V. Chantarangkul, M. Clerici, C. Bressi, P. L. A. Giesen, A. Tripodi, *Haematologica* **2003**, *88*, 547 – 554; b) Y. Dargaud, S. Béguin, A. Lienhart, R. Al Dieri, C. Trzeciak, J. C. Bordet, H. C. Hemker, C. Negrier, *Thromb. Haemostasis* **2005**, *93*, 475 – 480.
[49] T. Siegemund, S. Petros, A. Siegemund, U. Scholz, L. Engelmann, *Thromb. Haemostasis* **2003**, *90*, 781 – 786.
[50] a) L. Rugeri, S. Béguin, C. Hemker, J. C. Bordet, R. Fleury, B. Chatard, C. Negrier, Y. Dargaud, *Haematologica* **2007**, *92*, 1639 – 1646; b) S. Béguin, I. Keularts, R. Al Dieri, S. Bellucci, J. Caen, H. C. Hemker, *J. Thromb. Haemostasis* **2004**, *2*, 170 – 176.
[51] a) S. Petros, T. Siegemund, A. Siegemund, L. Engelmann, *Blood Coagulation Fibrinolysis* **2006**, *17*, 131 – 137; b) S. L. Boström, G. F. H. Hansson, T. C. Sarich, M. Wolzt, *Thromb. Res.* **2004**, *113*, 85 – 91.
[52] H. C. Hemker, S. Béguin, *Thromb. Haemostasis* **1995**, *74*, 134 – 138.
[53] A. S. Wolberg, *Thromb. Res.* **2007**, *119*, 663 – 665.
[54] T. Baglin, *Br. J. Haematol.* **2005**, *130*, 653 – 661.
[55] More on inner-filter effects: S. P. Srinivas, R. Mutharasan, *Biotechnol. Bioeng.* **1987**, *30*, 769 – 774.
[56] R. Wagenvoord, P. W. Hemker, H. C. Hemker, *J. Thromb. Haemostasis* **2006**, *4*, 1331 – 1338.
[57] a) S. Butenas, K. G. Mann, *J. Thromb. Haemostasis* **2007**, *5*, 1084 – 1085; b) H. C. Hemker, E. de Smedt, *J. Thromb. Haemostasis* **2007**, *5*, 1085 – 1087.
[58] As a result of competition between the substrate and natural enzyme inhibitors, the ETP, as a rule, is increased by the presence of substrate.
[59] H. C. Hemker, R. Al Dieri, S. Béguin, *Curr. Opin. Hematol.* **2004**, *11*, 170 – 175.
[60] H. C. Hemker, P. W. Hemker, R. Al Dieri, *Thromb. Haemostasis* **2009**, *101*, 171 – 177.
[61] V. Regnault, S. Béguin, T. Lecompte, *Pathophysiol. Haemostasis Thromb.* **2003**, *33*, 23 – 29.

Received: November 25, 2011
Revised: January 2, 2012
Published online on January 31, 2012

